Supplementary Information

Electrochemical conversion of 5-hydroxymethylfurfural over CuNi bimetallic catalyst: the synergistic of interfacial active sites

Yiwei Zhao[a], Chao Zhang[a], Shuangxi Xing*[b], Zuhang Jin[a], and Tingting Xiao[c]*

[a] School of Environment, Northeast Normal University, Changchun 130117, PR China.

[b] Faculty of Chemistry, Northeast Normal University, Changchun 130024, PR China.

[c] State Key Laboratory of Electroanalytical Chemistry, Changchun Institute of Applied Chemistry, Chinese Academy of Sciences, Changchun 130022, PR China

[*] Corresponding authors at: School of Environment, Northeast Normal University, Changchun 130117, PR China.

Email addresses: E-mail: zhangc614@nenu.edu.cn, and xingsx737@nenu.edu.cn

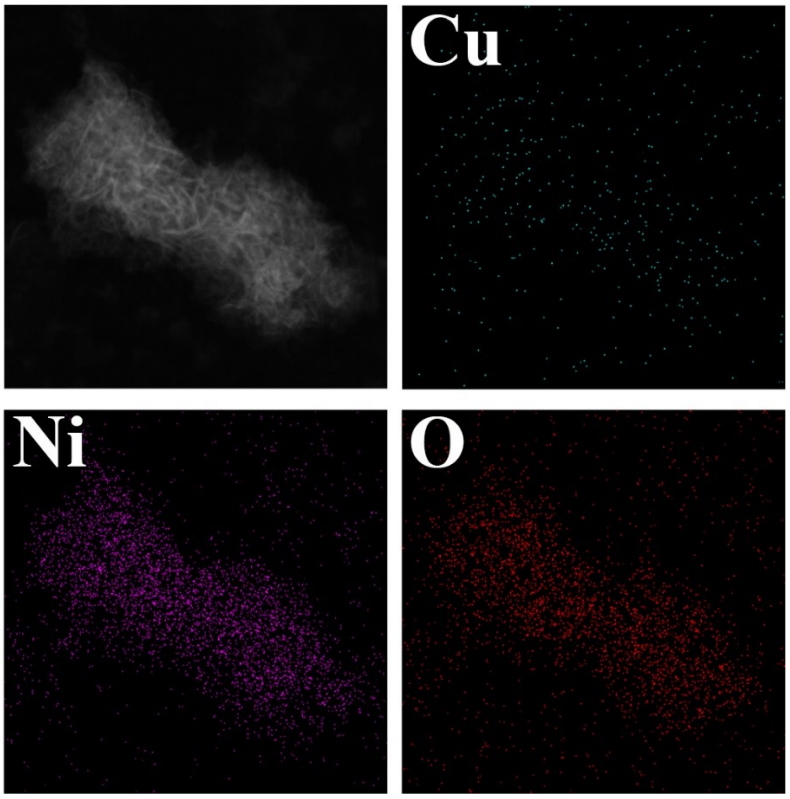

Fig. S1. Elemental maps of Cu, Ni, O of $Ni(OH)_2$-NCF.

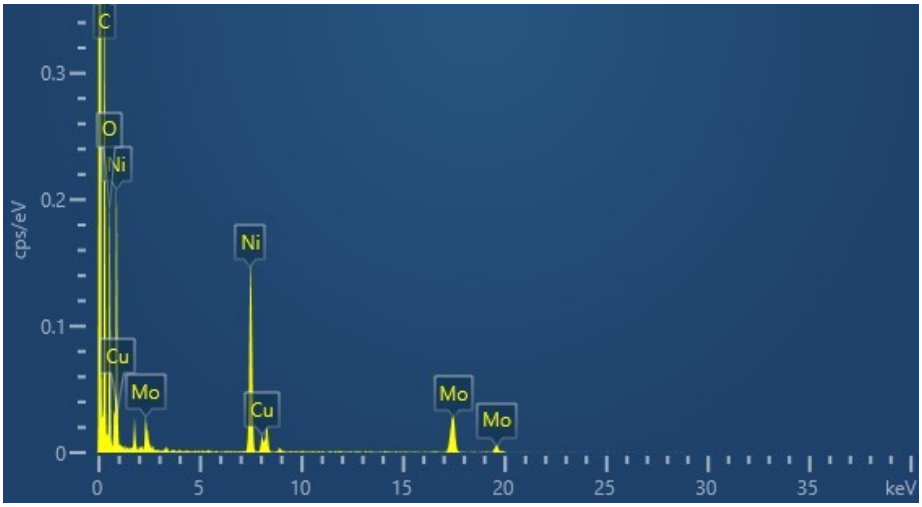

Fig. S2. Energy-dispersive spectroscopy spectrum of $Ni(OH)_2$-NCF.

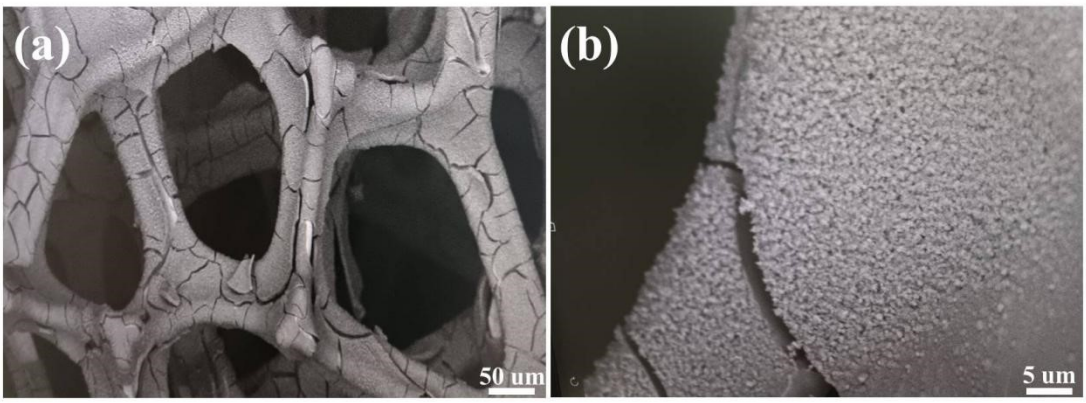

Fig. S3. SEM images of $Ni(OH)_2$-NCF: (a) high magnification; (b) low magnification.

Table S1. ICP test of Ni content before and after deposition of $Ni(OH)_2$-NCF-900.

	Before deposition	**After deposition**
Ni content in solution	9.68 ug/mL	4.88 ug/mL

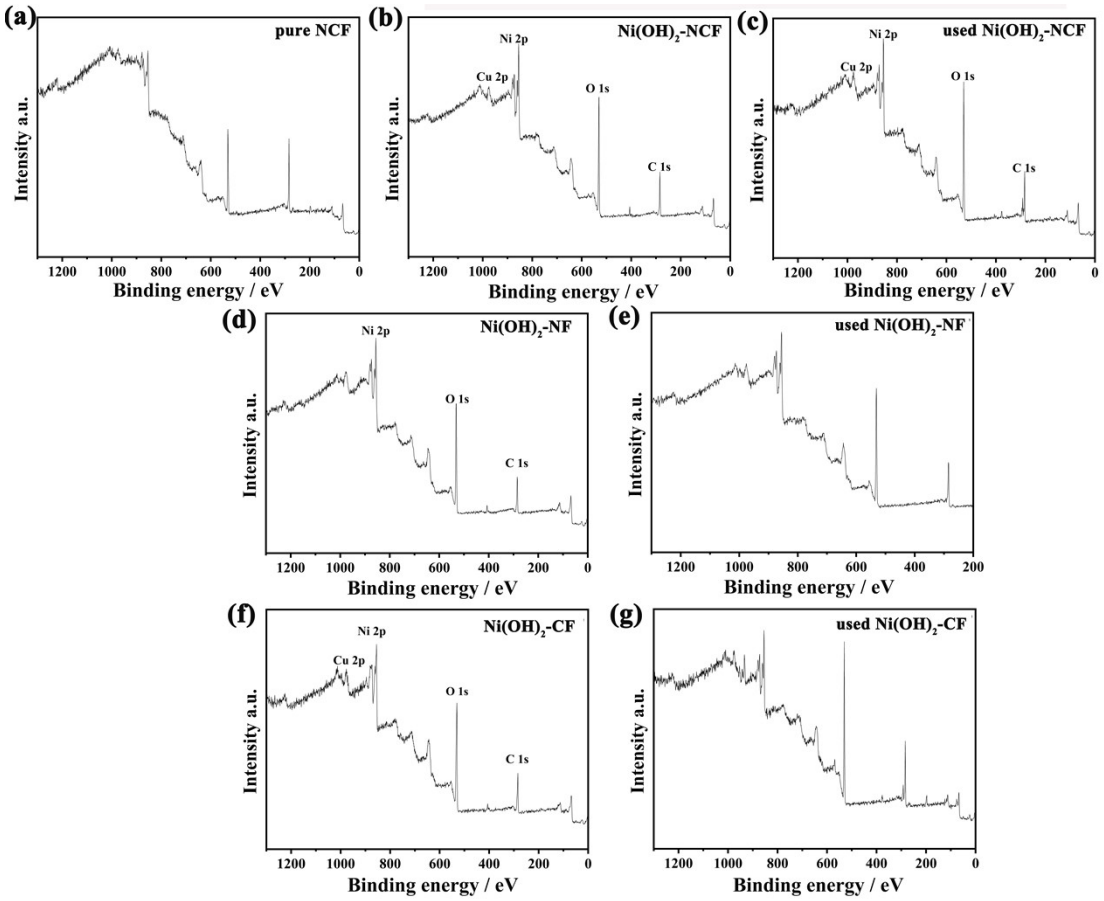

Fig. S4. XPS survey spectra of the catalysts: (a) pure NCF; (b) $Ni(OH)_2$-NCF; (c) used $Ni(OH)_2$-NCF; (d) $Ni(OH)_2$-NF; (e) used $Ni(OH)_2$-NF; (f) $Ni(OH)_2$-CF; (g) used $Ni(OH)_2$-CF.

Table S2. XPS O 1s components of the different electrocatalysts.

Electrocatalysts	**O I (%)**	**O II (%)**	**O III (%)**
$Ni(OH)_2$-NCF	25	51	24
$Ni(OH)_2$-NF	11	58	31
$Ni(OH)_2$-CF	23	57	20

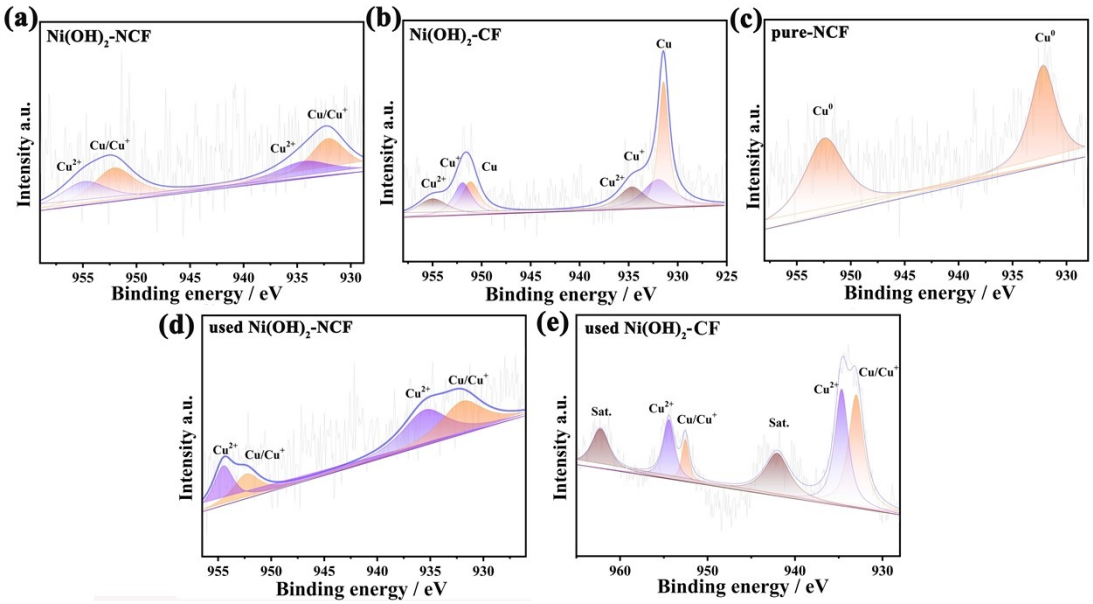

Fig. S5. The XPS Cu 2p spectra of the catalysts: (a) $Ni(OH)_2$-NCF; (b) $Ni(OH)_2$-CF; (c) pure-NCF; (d) used $Ni(OH)_2$-NCF; (e) used $Ni(OH)_2$-CF.

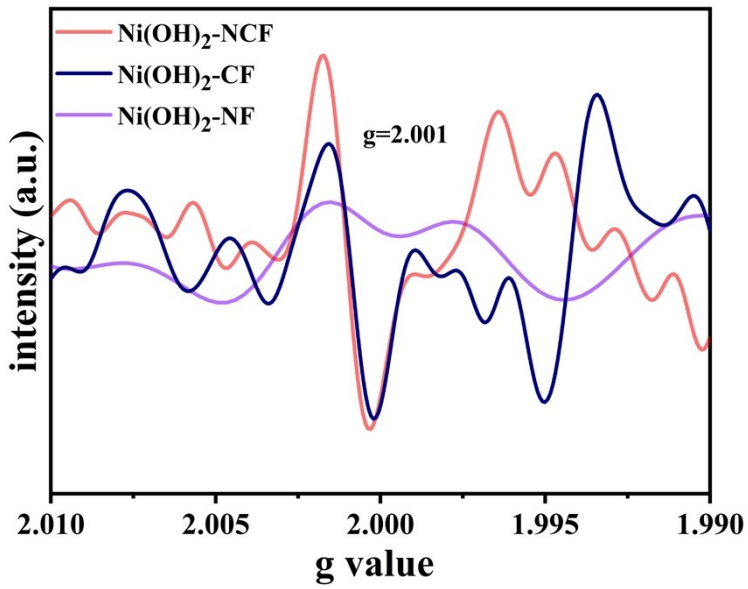

Fig. S6. EPR spectra of $Ni(OH)_2$-NCF, $Ni(OH)_2$-NF and $Ni(OH)_2$-CF.

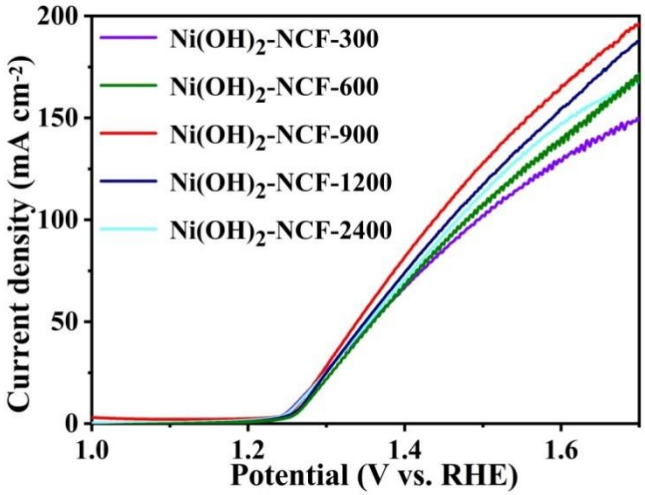

Fig. S7. LSV curves of the catalysts with 10 mM HMF in 1 M KOH.

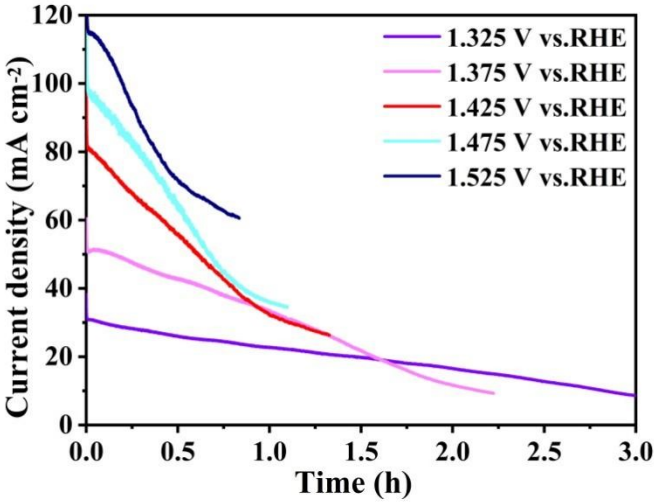

Fig. S8. Chronoamperometric curves of $Ni(OH)_2$-NCF under different potentials.

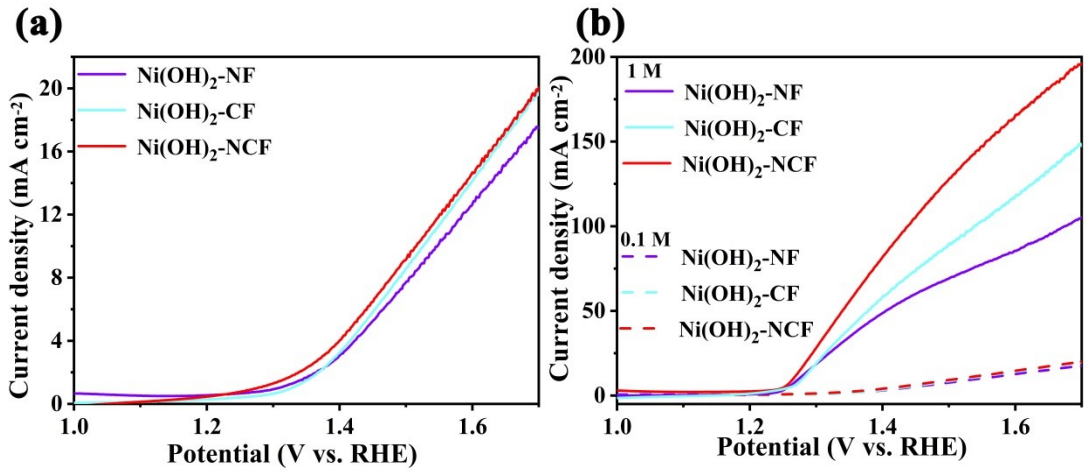

Fig. S9. (a) LSV curves (no compensation) of $Ni(OH)_2$-NCF, $Ni(OH)_2$-NF, and $Ni(OH)_2$-CF with 10 mM HMF in 0.1 M KOH; (b) Comparison of LSV curves of catalysts with HMF in 1 M and 0.1 M KOH.

Table S3. Current density and electrocatalytic performance of different electrocatalysts for HMFOR.

Entry	Catalysts	Current density (mA/cm^2)	Potential (vs. RHE)	KOH	FDCA yield (%)	FE (%)	Ref.
1	CF-$Cu(OH)_2$	55	1.82 V	1 M	98.7	100	[1]
2	Cu_xS@NiCo-LDHs	87	1.3	1 M	100	99	[2]
3	NiCu NTs	136	1.424	1 M	99	99	[3]
4	CF-CuO/Ni-BTC MOF	47.6	1.475	1 M	99.9	91.0	[4]
5	Ni_xSe_y–NiFe LDH@NF	135	1.423	1 M	99.3	98.9	[5]
6	Ni_3S_2-MoS_2/NF	68	-	1 M	93-96	100	[6]
7	Cr-$Ni(OH)_2$/NF	230	-	1 M	98	96	[7]
8	NF@$Ni_{0.85}Se$	50	1.5	1 M	-	95	[8]
9	Ni_3N@C	50	1.38	1 M	98	-	[9]
10	$Ni(OH)_2$-NCF	93.2	1.425	1 M	99	98.5	This work

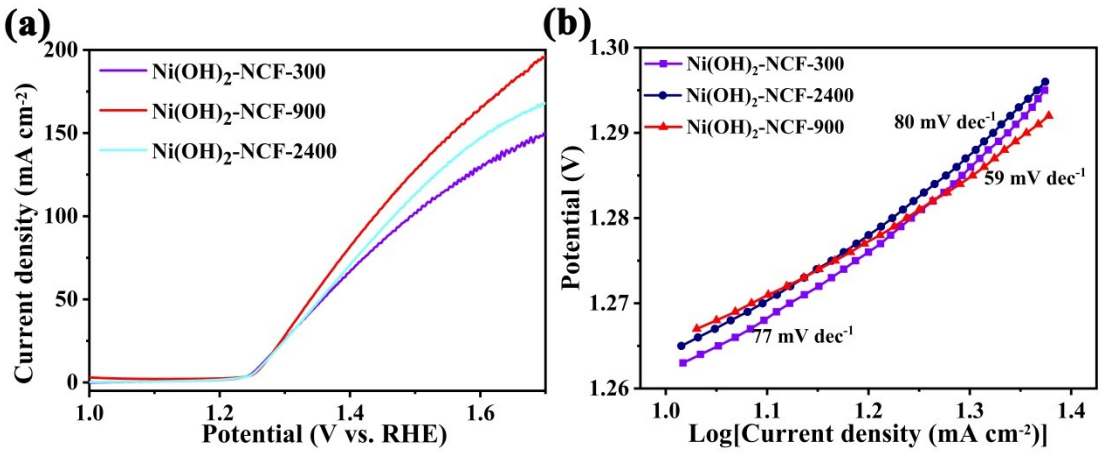

Fig. S10. (a) LSV curves of the catalysts with 10 mM HMF in 1 M KOH, (b) Tafel slope of the catalysts.

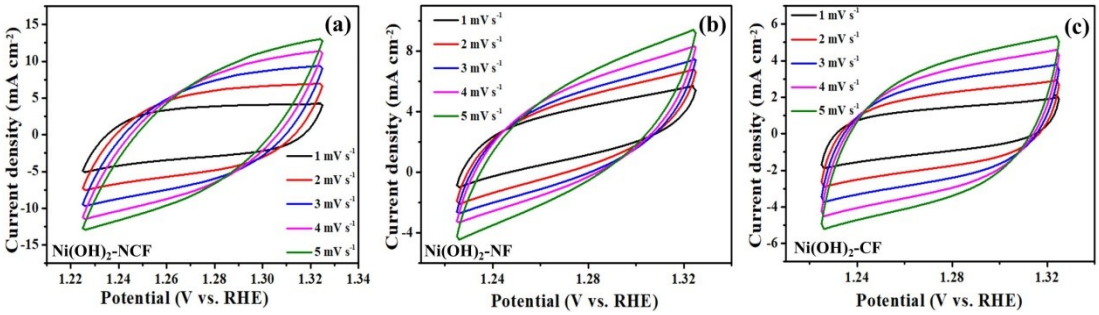

Fig. S11. C_{dl} of $Ni(OH)_2$-NCF, $Ni(OH)_2$-NF, and $Ni(OH)_2$-CF measured by CVs in 1 M KOH with 10 mM HMF with a scan rate of 1 to 5 mV/s.

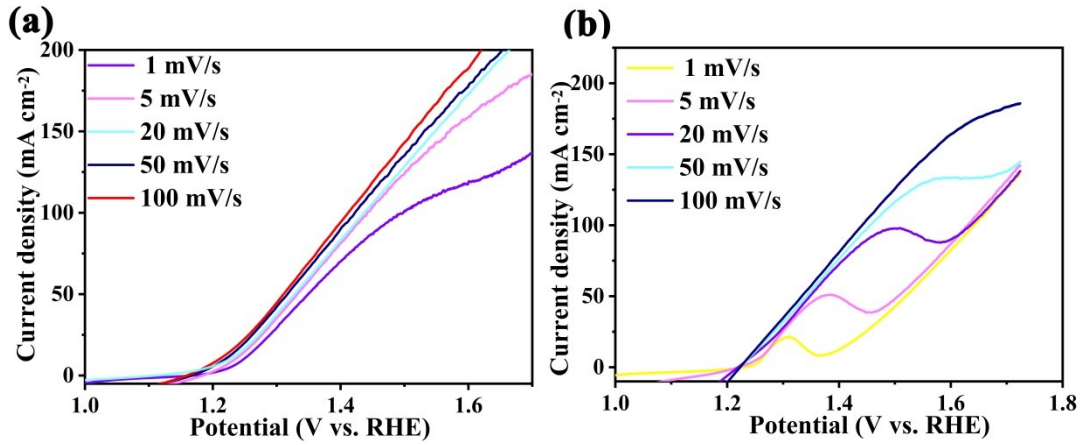

Fig. S12. (a) HMFOR process on $Ni(OH)_2$-NCF with different scan rates; (b) OER process on $Ni(OH)_2$-NCF with different scan rates.

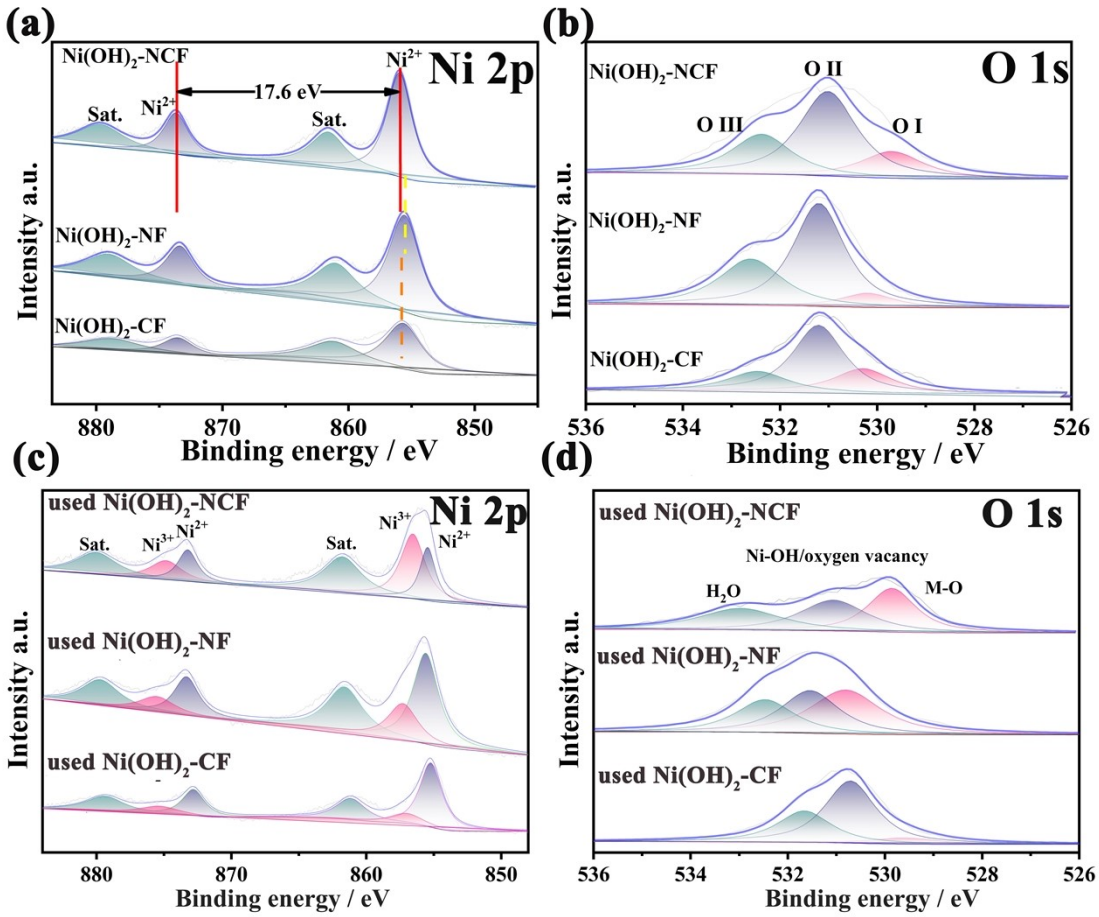

Fig. S13. XPS results of the fresh and used $Ni(OH)_2$-NCF, $Ni(OH)_2$-NF, and $Ni(OH)_2$-CF catalysts for HMFOR: (a) Ni 2p and (b) O 1s.

Table S4. XPS Ni 2p components of the different electrocatalysts.

Electrocatalysts	**Ni^{3+}(%)**	**Ni^{2+}(%)**	**Ni^{0}(%)**
Used-$Ni(OH)_2$-NCF	60.2	39.7	0
Used-$Ni(OH)_2$-NF	32.5	67.5	0
Used-$Ni(OH)_2$-CF	22.5	77.5	0

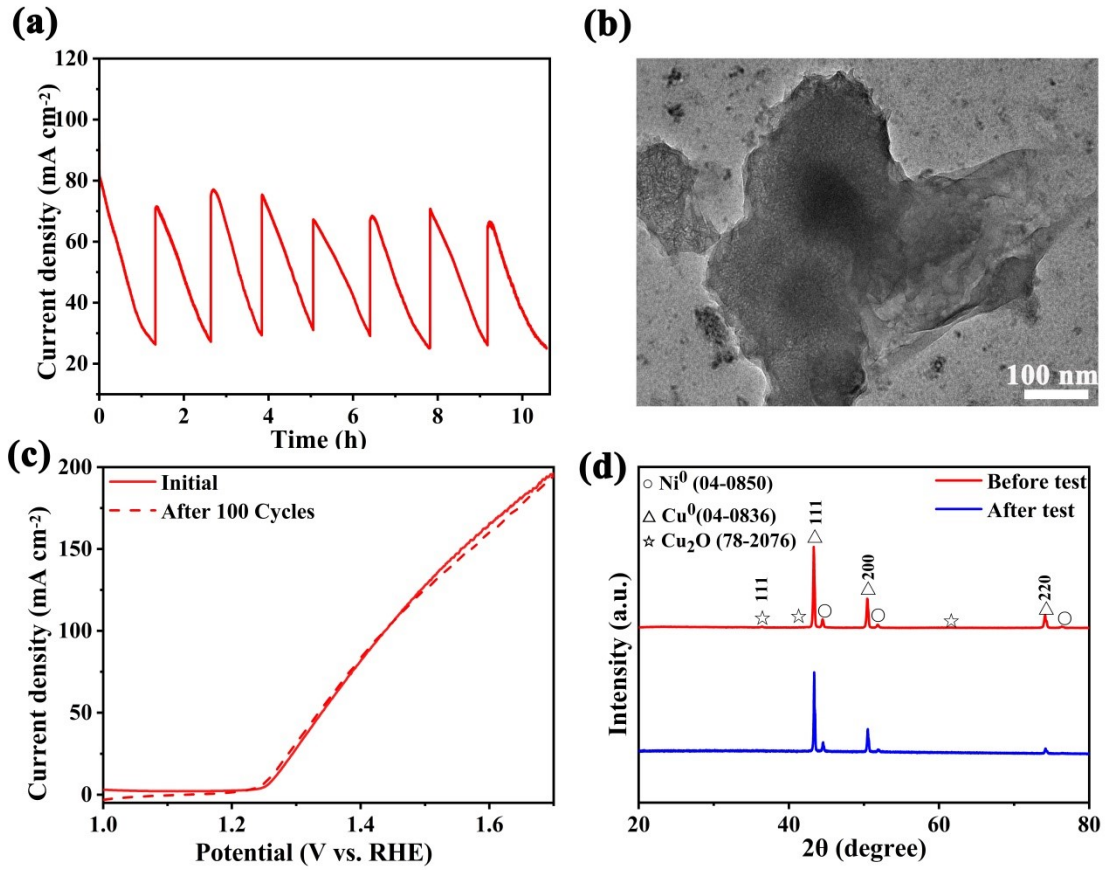

Fig. S14. (a) Consecutive 8 runs of HMFOR at a constant voltage of 1.425 V with the intermittent addition of 10 mM HMF; (b) TEM of the $Ni(OH)_2$-NCF after recycling; (c) LSV curve of $Ni(OH)_2$-NCF after 100 cycles (All test in 1 M KOH containing 10 mM HMF); (d) The XRD of $Ni(OH)_2$-NCF before and after HMFOR.

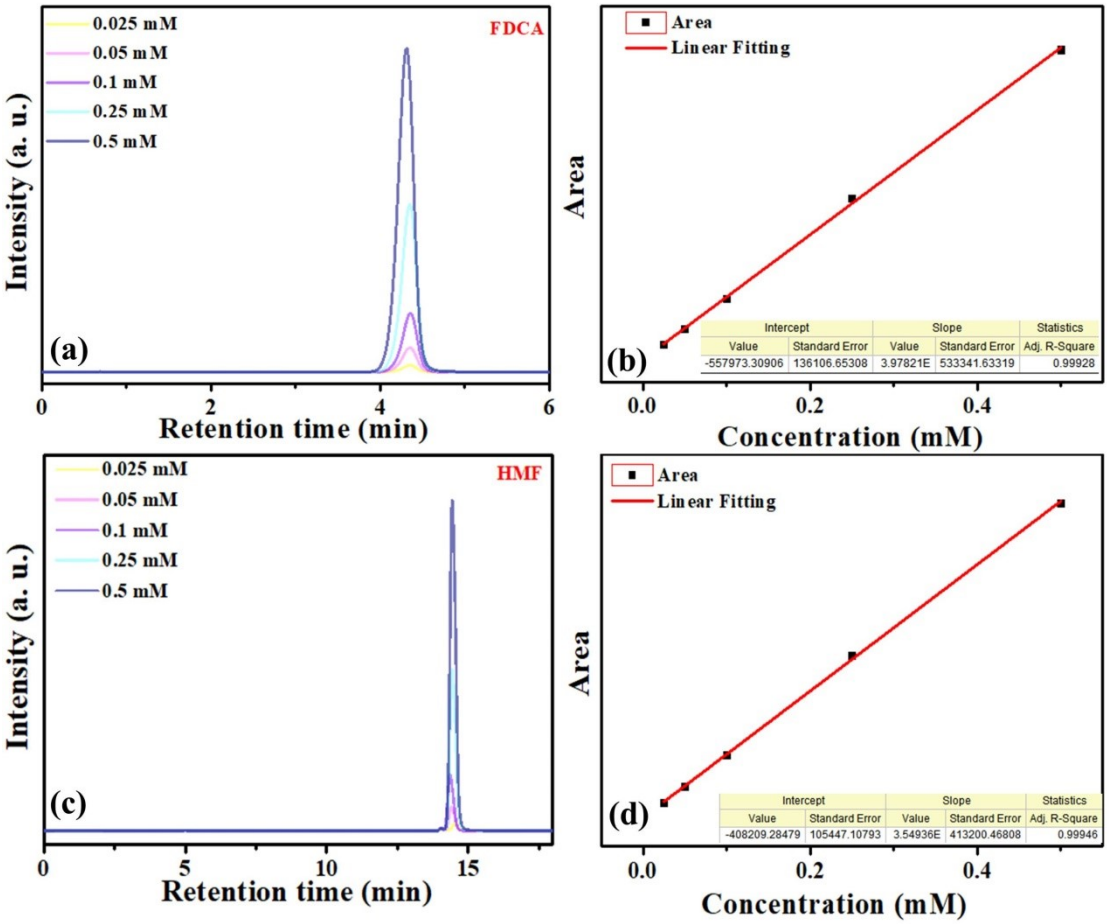

Fig. S15. HPLC analysis results and the standard curves: (a) and (b) FDCA; (c) and (d) HMF.

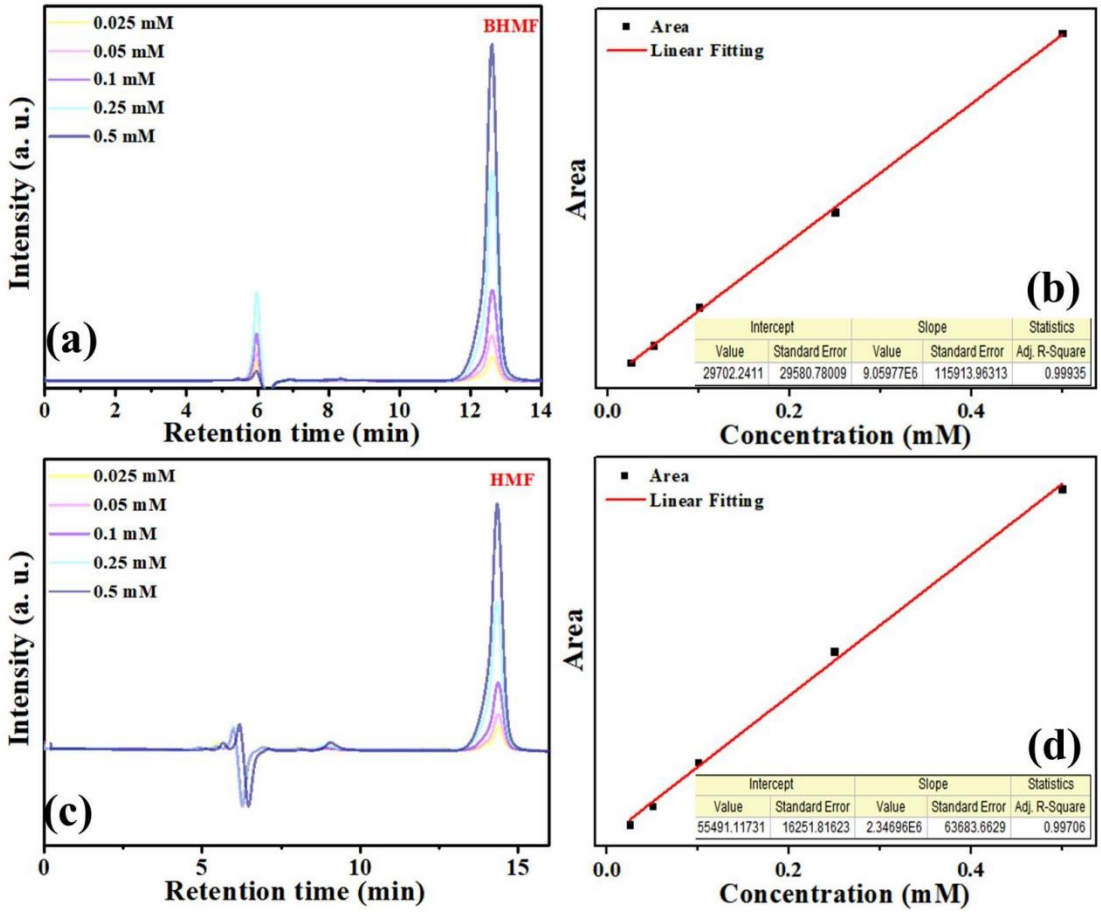

Fig. S16. HPLC analysis results and the standard curves: (a), (b) BHMF; (c), (d) HMF.

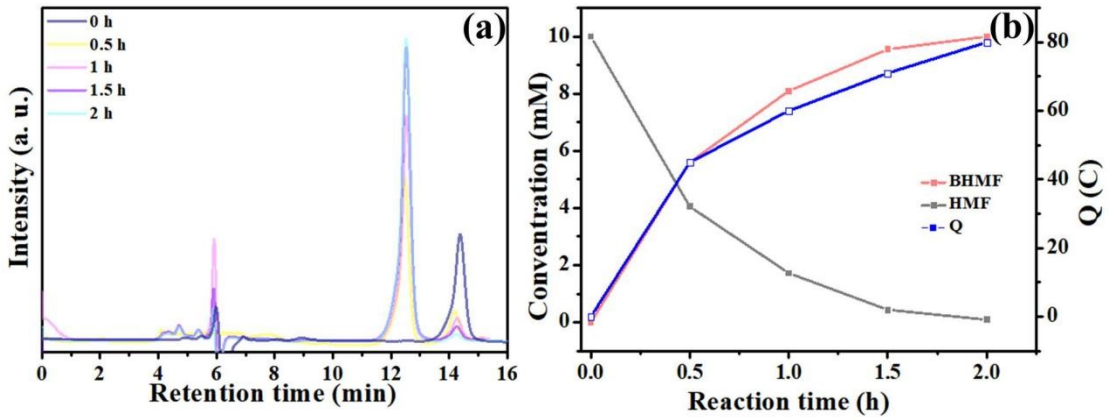

Fig. S17. (a) HPLC results of HMFRR on Cu-NCF at -0.275 V; (b) The concentration changes of HMF and BHMF during the HMFRR.

REFERENCES

1. X. Pang, H. Bai, H. Zhao, W. Fan and W. Shi, Efficient electrocatalytic oxidation of 5-hydroxymethylfurfural coupled with 4-nitrophenol hydrogenation in a water system, *ACS Catal.*, 2022, **12**, 1545-1557.
2. X. Deng, X. Kang, M. Li, K. Xiang, C. Wang, Z. Guo, J. Zhang, X.-Z. Fu and J.-L. Luo, Coupling efficient biomass upgrading with H_2 production via bifunctional Cu_xS@NiCo-LDH core–shell nanoarray electrocatalysts, *J. Mater. Chem. A*, 2020, **8**, 1138-1146.
3. L. Zheng, Y. Zhao, P. Xu, Z. Lv, X. Shi and H. Zheng, Biomass upgrading coupled with H_2 production via a nonprecious and versatile Cu-doped nickel nanotube electrocatalyst, *J. Mater. Chem. A*, 2022, **10**, 10181-10191.
4. X. Pang, H. Bai, Y. Huang, H. Zhao, G. Zheng and W. Fan, Mechanistic insights for dual-species evolution toward 5-hydroxymethylfurfural oxidation, *J. Catal.*, 2023, **417**, 22-34.
5. Y. Zhong, R.-Q. Ren, J.-B. Wang, Y.-Y. Peng, Q. Li and Y.-M. Fan, Grass-like NixSey nanowire arrays shelled with NiFe LDH nanosheets as a 3D hierarchical core-shell electrocatalyst for efficient upgrading of biomass-derived 5-hydroxymethylfurfural and furfural, *Catal. Sci. Technol.*, 2022, **12**, 201-211.
6. S. Yang, Y. Guo, Y. Zhao, L. Zhang, H. Shen, J. Wang, J. Li, C. Wu, W. Wang, Y. Cao, S. Zhuo, Q. Zhang and H. Zhang, Construction of Synergistic Ni_3S_2-MoS_2 Nanoheterojunctions on Ni Foam as Bifunctional Electrocatalyst for Hydrogen Evolution Integrated with Biomass Valorization, *Small*, 2022, **18**, 2201306.
7. Z. Yang, B. Zhang, C. Yan, Z. Xue and T. Mu, The pivot to achieve high current density for biomass electrooxidation: Accelerating the reduction of Ni^{3+} to Ni^{2+}, *Appl. Catal., B*, 2023, **330**, 122590.
8. C. Yang, C. Wang, L. Zhou, W. Duan, Y. Song, F. Zhang, Y. Zhen, J. Zhang, W. Bao, Y. Lu, D. Wang and F. Fu, Refining d-band center in $Ni_{0.85}Se$ by Mo doping: a strategy for boosting hydrogen generation via coupling electrocatalytic oxidation 5-hydroxymethylfurfural, *Chem. Eng. J.*, 2021, **422**, 130125.
9. N. Zhang, Y. Zou, L. Tao, W. Chen, L. Zhou, Z. Liu, B. Zhou, G. Huang, H. Lin and S. Wang, Electrochemical Oxidation of 5-Hydroxymethylfurfural on Nickel Nitride/Carbon Nanosheets: Reaction Pathway Determined by In Situ Sum Frequency Generation Vibrational Spectroscopy, *Angew. Chem. Int. Ed.*, 2019, **58**, 15895-15903.